Title: Position-specific carbon isotope fingerprinting of fluorinated organics and degradation products

Cornelia Rasmussen[1] and David W. Hoffman[2]*

[1]University of Texas Institute for Geophysics, Jackson School of Geosciences, University of Texas at Austin, 10601 Exploration Way, Austin, TX 78758. (crasmussen@utexas.edu)

[2]Department of Molecular Biosciences, College of Natural Science, University of Texas at Austin, 100 E 24th St, Austin, TX 78712. (dhoffman@mail.utexas.edu)

*Corresponding author

Abstract

Fluorinated organic compounds are of growing environmental and forensic relevance due to their widespread use in pharmaceuticals, agrochemicals, and consumer products, their environmental persistence, and potential ecological and human health impacts. Elucidating their sources and transformation pathways is therefore a major focus of current research. Stable carbon isotope analysis provides a powerful approach for tracing molecular origins and linking parent compounds to degradation products. Recent isotope measurements have largely relied on mass-spectrometry techniques, which provide only an average isotope ratio across a compound. Here, we employ a novel nuclear magnetic resonance (NMR) spectroscopy tool to determine position-specific carbon isotope ratios ($^{13}C/^{12}C$) in organofluorine compounds and their degradation products. This approach enables isotope measurements without combustion or extensive purification and, crucially, resolves ratios at individual carbon positions rather than bulk averages. The resulting intramolecular isotope fingerprints are unique to a molecule's source. Applied to selected pharmaceuticals and pesticides, these fingerprints allow discrimination of chemically identical compounds. Moreover, we show that the $^{13}C/^{12}C$ signature at the fluorinated carbon persists through degradation, demonstrated for lansoprazole and fipronil. The ^{19}F NMR data produced for the $^{13}C/^{12}C$ analyses are also well suited for impurity profiling, providing an additional dimension for fingerprinting fluorinated organics. These findings suggest that position-specific isotope analysis can serve as part of a broader suite of tools for source characterization of organofluorine compounds and their breakdown derivates, with potential applications in product validation, forensics, and linking these compounds to their breakdown products.

INTRODUCTION

The substitution of fluorine atoms into organic molecules represents a significant advancement in the chemical sciences, supporting innovation in drug, agrochemical, and materials developmen[1,2]. For example, a large fraction of the pharmaceuticals used in human medicine contain one or more fluorine substitutions, enhancing efficacy and bioavailability[3-7]. Fluorinated molecules are widely used in herbicides, insecticides and fungicides, where the fluorine substitution improves effectiveness and

resistance to degradation in the environment[8,9]. In addition, fluorinated organics are incorporated into a wide range of industrial and consumer products, such as firefighting foams, coatings and surfactants[1,10].

The strength of the C-F chemical bonds are both a feature and a bug. They can make molecules resistant to chemical and metabolic breakdown, however this exceptional stability can lead to their accumulation in the environment, with potential impacts on human, wildlife, and ecosystem health[1,7,11-17]. Organofluorine molecules are now ubiquitous, and have been detected in human blood plasma worldwide and in various wildlife, ranging from invertebrates to large mammals[10,18-20]. As a result, there is a scientific and regulatory interest in monitoring, tracking, and quantifying these molecules in air, water, soil, wildlife, and humans. Beyond detection, there is also a growing emphasis on source attribution to identify whether organofluorine pollution comes from industrial processes, consumer products, pharmaceuticals, or other origins. The widespread use of organofluorine molecules in pharmaceuticals creates a need for additional forensic capabilities, for product validation and counterfeit detection. These interests emphasize the need for novel analytical approaches capable of tracing sources, transformation pathways and degradation products[15-19].

Here, we introduce novel nuclear magnetic resonance (NMR) spectroscopy tools for obtaining position-specific carbon isotope ratios ($^{13}C/^{12}C$) in a set of organofluorine compounds and their degradation products. Unlike traditional isotope ratio mass spectrometry (IRMS), which measures the average isotopic composition of a sample or molecule, position-specific $^{13}C/^{12}C$ analysis provides isotope ratios for chemically distinct carbon positions within the molecular structure. This position-specific information provides more information than traditional IRMS, and can produce a unique intramolecular isotope fingerprint that can reveal differences in molecular origin[21-24]. Differences in the intramolecular distribution of ^{12}C and ^{13}C can distinguish molecules that are otherwise chemically identical, providing a potential link to the source and insight into how a molecule was produced[24-25].

Although fluorine (^{19}F) NMR has been widely used to identify and quantify organofluorine molecules in mixtures[26-31], its application to $^{13}C/^{12}C$ isotope analysis is relatively recent[32]. Position-specific $^{13}C/^{12}C$ analyses of organofluorine molecules have been limited to essentially pure molecules, or mixtures where the ^{19}F NMR signals are completely resolved from other components[32]. In the present work, we address this limitation, making position-specific $^{13}C/^{12}C$ analysis possible for a wider range of samples, including those with NMR signals that overlap with the molecule of interest, and mixtures of fluorinated organics and their degradation products.

The organofluorine molecules that analyzed here include representative pharmaceuticals and insecticides, and mixtures containing their degradation products. We analyze samples of paroxetine (a selective serotonin reuptake inhibitor, or SSRI) from different sources, lansoprazole (a proton pump inhibitor that reduces stomach acid), and the insecticides fipronil and bifenthrin. We illustrate that chemically identical organofluorine molecules can be distinguished based on their intramolecular $^{13}C/^{12}C$ distribution, even when they are part of the complex mixture. Using lansoprazole and fipronil, we show that the $^{13}C/^{12}C$ isotopic fingerprint is carried from the parent molecule into its degradation products.

EXPERIMENTAL SECTION

Samples and sample preparation. The samples were dissolved in 0.7 mL of NMR solvent, 99.8% $CDCl_3$, 99.8% CD_3OD or 99.9% d6-DMSO, all acquired from Cambridge Isotope Laboratories. Approximately 1 to 2 microliters of a 5 mg/mL chromium (III) acetylacetonate solution in NMR solvent

was titrated into samples, to reduce the longest T_1 relaxation times of the detected nucleus to 1 to 1.3 seconds.

Paroxetine was obtained from two sources. Paroxetine certified reference material (pharmaceutical secondary standard, source LRAD4389, 20 mg) from Sigma-Aldrich was dissolved in CD_3OD. Paroxetine was also obtained by crushing tablets of Paxil, mixing with CD_3OD, followed by centrifugation and collecting the supernatant to produce a sample.

Lansoprazole was purchased as a certified reference material (pharmaceutical secondary standard PHR1390, source LRAD7178, 15 mg) from Millipore-Sigma. In addition, Lansoprazole capsules ("Up&Up" and "Prevacid") were obtained from a local drug store, crushed, and dissolved for NMR analysis (~15 mg of analyte per sample). Degradation of lansoprazole occurred spontaneously in the NMR tube, and was monitored by obtaining spectra over a period of weeks; degradation was nearly complete after 14 days.

Bifenthrin analytical standard (Pestanal batch BCCG1821, 20 mg) was obtained from Sigma-Aldrich. Ortho Flea Killer containing 0.25% bifenthrin was purchased at a local hardware store; 0.2 L of the flea killer liquid was mixed with 20 mL $CDCl_3$, shaken, and the $CDCL_3$ phase was collected, dried, and redissolved in $CDCl_3$ to produce an NMR sample.

Fipronil was purchased from Sentry Fiproguard for dogs (lot P006107) and diluted into $CDCl_3$ to produce an NMR sample with ~20 mg fipronil. For fipronil degradation experiments, 1 mL of Fiproguard insecticide was placed in a Bockel UV cross-linking chamber (model 234100), and exposed to UV light with wavelengths near 254 nm for 16 to 40 hours; 0.1 mL of the degradation mixture was mixed with 0.6 mL $CDCl_3$ for NMR analysis.

NMR data collection. Analyses were performed using a Varian VNMRS 600 MHz spectrometer equipped with a broadband 5 mm AutoXDB PFG probe ($^1H/^{19}F$ coil external to the ^{13}C coil) and temperature control. NMR spectra were acquired at a regulated temperature of 25 ºC using a pulse sequence (Figure S9) designed to minimize temperature fluctuations due to ^{13}C decoupling[23]. Data sets consisted of stacks of typically 64 to 200 consecutively acquired ^{19}F or ^1H spectra of 8 to 32 scans each, alternating with and without ^{13}C decoupling during the acquisition time. Total acquisition times ranged from 4 hours to overnight runs for each data set. The delay between individual scans exceeded ten times the longest T_1 relaxation time of the detected nucleus (either ^{19}F or ^1H), determined by inversion-recovery. Spectra were obtained without sample spinning to avoid spinning sidebands.

NMR data processing. Raw NMR data were processed using MestReNova software[33] for apodization, zero filling, Fourier transformation, and an initial phase correction. Each free induction decay (FID) was zero-filled to two million points and multiplied by a combination of a decaying exponential and a shifted sine-squared function to produce a relatively flat baseline and minimize truncation artifacts; acquisition time for each FID was 0.64 sec, which provided sufficient spectral resolution without excessive heating during ^{13}C decoupling (Fig. S9). The spectral region containing the central (^{19}F-^{12}C or ^1H-^{12}C) and satellite (^{19}F-^{13}C or ^1H-^{13}C) peaks was then exported from MestReNova in CSV format.

An R script was used to separately align the alternating ^{13}C-coupled and decoupled spectra, which were then used together to isolate the signals of interest from those of overlapping impurities. Signals from the ^{19}F (or ^1H) nuclei coupled to ^{13}C were obtained by subtracting the ^{13}C-decoupled spectrum from the ^{13}C-coupled spectrum, with corrections for shim or phase mismatch between spectra, and the ^{13}C isotope shift in the impurity signals, which causes ^{19}F-^{13}C to collapse to frequencies that are offset from the corresponding ^{19}F-^{12}C peaks upon decoupling. This procedure effectively separates the NMR signals from ^{19}F with bonds to ^{13}C from those with bonds to ^{12}C (Fig. 1).

Using an R script, pairs ^{19}F-^{13}C satellite peaks (Peak 2 and Peak 3 in Eq. 1) were aligned point-by-point and summed, and then digitally superimposed onto the corresponding central ^{19}F-^{12}C peak (Peak 1 in Eq. 1). Four variables were then used to obtain the best fit to Eq. 1: the absolute $^{13}C/^{12}C$ ratio (*Ratio*), a line broadening correction (*LB*), and corrections for baseline offset and slope (*b0* and *b1*):

$$(\text{Peak 2} + \text{Peak 3}) = (\text{Peak 1} \times LB \times Ratio) + b1 \times x + b0 \qquad \text{(eq. 1)}$$

LB is a Lorentzian line broadening factor that is used to match the widths of the central (^{19}F-^{12}C) and satellite (^{19}F-^{13}C) peaks; this accounts for the slight broadening of the satellite peaks due to the additional relaxation pathway that is introduced by the ^{13}C nucleus. The fitting was carried out using the non-linear least squares Levenberg-Marquardt (nlsLM) algorithm in R. This approach provided a robust framework for determining the $^{13}C/^{12}C$ ratio by aligning and superimposing peak shapes, while simultaneously correcting for the ^{13}C isotope shift, the line width difference between the central and satellite peaks, and minor baseline variations. After initial peak shape fitting, the stack of consecutively acquired spectra was systematically searched for outliers, results were cross validated across the stack of spectra, and an average and standard deviation was calculated for the fitted parameters. The $^{13}C/^{12}C$ ratios provided by the analysis of the NMR spectra were converted to $\delta^{13}C_{VPDB}$. A map of the workflow for obtaining position-specific $\delta^{13}C_{VPDB}$ from the NMR spectra is provided in the supporting information (Fig. S1), along with the raw NMR data, and complete R scripts for processing the data.

RESULTS AND DISCUSSION

The ^{19}F NMR-based method introduced here enables the determination of the intramolecular carbon isotope variability in organofluorine compounds, despite the presence of impurities and NMR signals that overlap with the ^{19}F-^{13}C satellite peaks (Figure 1). This capability represents a significant advance, because samples are often complex mixtures rather than pure substances. The ability to perform position-specific $^{13}C/^{12}C$ analysis with minimal pre-separation is important, as purification steps such as column chromatography can alter the sample and/or introduce isotopic fractionation (Holtvoeth et al., 2019)[34]. Moreover, this approach allows for the $^{13}C/^{12}C$ analysis of multiple compounds within the same mixture, including degradation products in the presence of the parent molecule.

We accomplish the separation of NMR signals of interest from those of impurities through the combined use of ^{13}C-coupled and ^{13}C-decoupled of ^{19}F NMR spectra, a data collection scheme that is routine on a modern NMR spectrometer and requires no special hardware. In the ^{19}F NMR spectra, fluorine atoms are coupled to ^{13}C nuclei (~1.1 % natural abundance) giving rise to two relatively smaller satellite peaks flanking the main ^{12}C-^{19}F signal (~98.9 % natural abundance). Applying ^{13}C-decoupling during acquisition collapses the ^{19}F-^{13}C satellite peaks into a central position, leaving the main ^{12}C-^{19}F signals unaffected and simplifying the spectrum. This allows us to observe the NMR signals of impurities and subtract them from the ^{13}C-coupled spectrum, leaving us with the signals associated with the carbon position of interest which can be superimposed to obtain a $^{13}C/^{12}C$ ratio (Figures 1, S2, S5, S6, S8). Separating the signals of the molecule of interest from those of impurities is essential, since even small peaks that overlap with the ^{19}F-^{13}C satellites will significantly degrade the shape fit when the sum of the satellites is superimposed onto the central peak. The $^{13}C/^{12}C$ ratio is determined from the scale factor for a shape superposition, exploiting the relationship between the shapes of the central and satellite peaks, which is essential in achieving the parts-per-thousand accuracy needed for $^{13}C/^{12}C$ isotope analysis[35].

In the absence of officially recognized $^{13}C/^{12}C$ reference materials for fluorinated organics, we used 2,2,2-trifluoroethanol as in house standard to validate the ^{19}F NMR-based method for position-specific $^{13}C/^{12}C$ isotope analysis using ^{13}C-coupled and decoupled spectra (Figure S8). The average and position-specific $^{13}C/^{12}C$ distributions in this molecule have previously been characterized by IRMS, ^{1}H NMR and ^{19}F NMR[32].

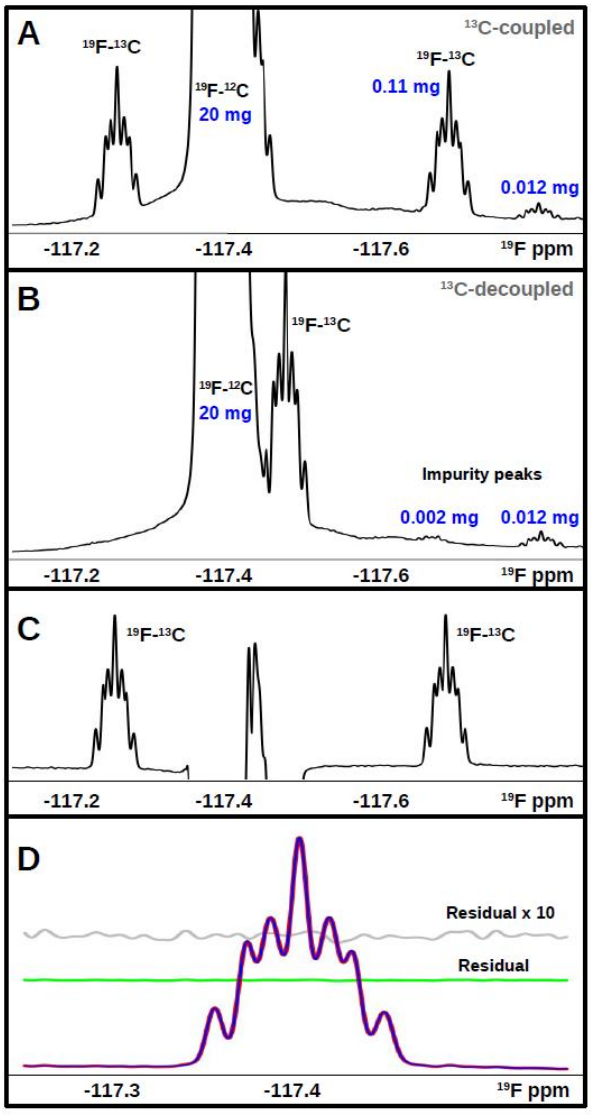

Figure 1: $^{13}C/^{12}C$ abundance at the C-F position of the paroxetine in crushed Paxil tablets, with 20 mg of paroxetine dissolved CD_3OD. (A) ^{19}F NMR spectrum obtained without ^{13}C decoupling during the acquisition time, with approximate mass associated with the NMR peaks; (B) ^{13}C-decoupled ^{19}F NMR spectrum, showing the collapse of the two ^{19}F-^{13}C satellite peaks to their central position, and exposing the impurity peaks so they can be subtracted; (C) difference spectrum obtained by subtracting panel A from panel B, after panel B has been corrected for field drift, phase drift and the isotope shift in the decoupled spectrum, as described in Figure S1; and (D) the sum of the two ^{19}F-^{13}C satellite peaks in panel C (red) superimposed onto the central ^{19}F-^{12}C peak in panel A (blue). The best fit to eq. 1 was achieved with a

$^{13}C/^{12}C$ isotope ratio of 0.010645, corresponding to $\delta^{13}C$ = -40.9‰. The residual (difference between the red and blue lines) and residual times ten are shown in green and gray, respectively, offset from the baseline for clarity.

Applying this ^{19}F NMR method for measuring $^{13}C/^{12}C$ ratios, we found that organofluorine molecules from different sources preserve unique position-specific carbon isotope fingerprints, allowing chemically identical molecules to be distinguished and linked to their source (Figures 2, 3, S8).

Many organofluorine compounds contain C-H bonds in addition to C-F bonds within their molecule structure. We therefore combined the ^{19}F NMR method introduced here with a previously developed ^{1}H NMR technique for position-specific $^{13}C/^{12}C$ analysis in the presence of overlapping impurity signals[23,24]. Used together, the ^{19}F and ^{1}H NMR techniques provided $^{13}C/^{12}C$ ratios at additional positions, resulting in more information per molecule, and a more robust carbon isotope fingerprint (Figure 2 & 3).

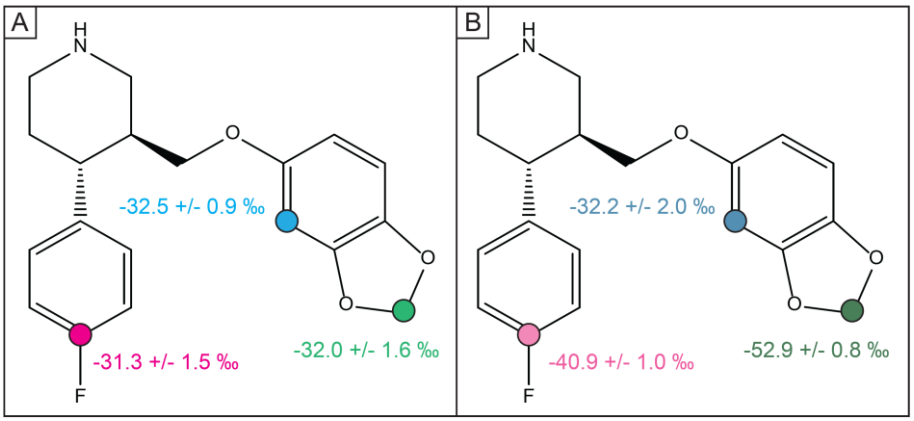

Figure 2: Position-specific $^{13}C/^{12}C$ abundance ($\delta^{13}C$) in (A) the paroxetine analytical standard and (B) a sample prepared from crushed Paxil tablets, stated in permil (‰) relative to VPDB with 2σ uncertainty. The C17 position (pink) was analyzed using ^{19}F NMR (Figure 1); the C6 and C7 positions (green and blue) were determined using ^{1}H NMR spectra obtained with and without ^{13}C decoupling (Figure S7).

Significantly, we found that the position-specific $^{13}C/^{12}C$ abundance is preserved for carbons in C-F bonds upon degradation of the source molecule (Figure S5, S7). This allows the method to be used to make source-sink correlations for a molecule and its degradation products (Figure 4). For this work, we degraded the insecticide fipronil with UV light[36], with the pyrazole-3-carbonitrile ring being a likely chromophore. Exposing fipronil to UV light results in the gradual disappearance of the fipronil trifluoromethylsulfoxide peak at -75 ppm in the ^{19}F spectrum, along with the appearance of a new peak at -57 ppm attributed to a degradation product (Figure 3, S4, S5). ^{19}F spectra indicate that the 2,6-dichloro-4-(trifluoromethyl)phenyl group (-63 ppm in the ^{19}F spectrum) is preserved during UV degradation (Figure S7). Position-specific isotope analysis shows that the $^{13}C/^{12}C$ ratio in the trifluoromethylsulfoxide in the fipronil source molecule is preserved in the UV degradation product, remaining at -43 ‰ (Figure 4A).

Lansoprazole, which exhibits a ^{19}F NMR resonance at -75 ppm, was observed to spontaneously degrade over several weeks to form 2,2,2-trifluoroethanol with a ^{19}F resonance at -78 ppm. ^{19}F NMR analysis (Figures 4B) showed that the position-specific $^{13}C/^{12}C$ ratio associated with the C-F bond in lansoprazole (-20.2 ‰) was preserved in the resulting 2,2,2-trifluoroethanol (Figure 4B and S3). The unchanged $^{13}C/^{12}C$ ratio at the fluorinated carbon indicates that the degradation process does not induce

measurable isotope fractionation at this position (because the C-F bond is preserved), and carbon isotope abundance can be used as a tool in linking the degradation product with its source molecule.

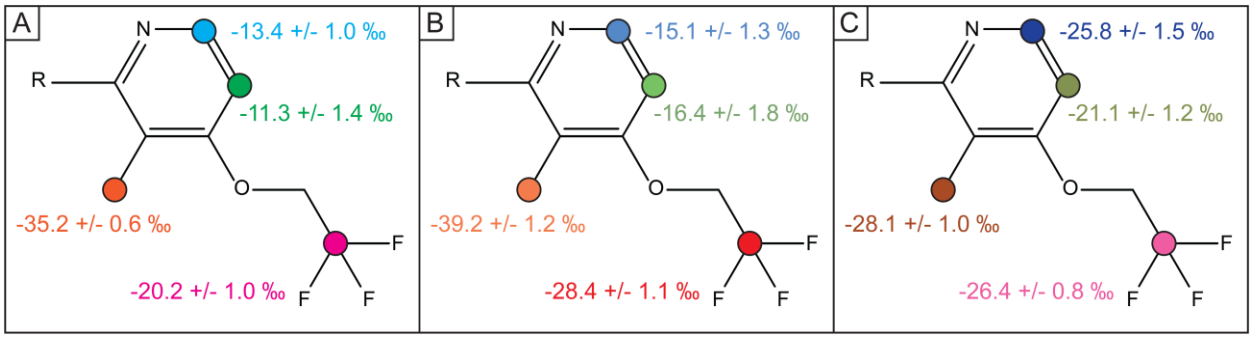

Figure 3: Position-specific $^{13}C/^{12}C$ abundance ($\delta^{13}C_{VPDB}$) in lansoprazole samples, determined by ^{19}F and ^{1}H NMR, stated in permil (‰) with 2σ uncertainty. Part of the lansoprazole structure is abbreviated as R. The full molecular structure can be found in Figure S2. (A) Lansoprazole analytical standard; (B) Up&Up brand lanzoprazole; (C) Lansoprazole from Prevacid.

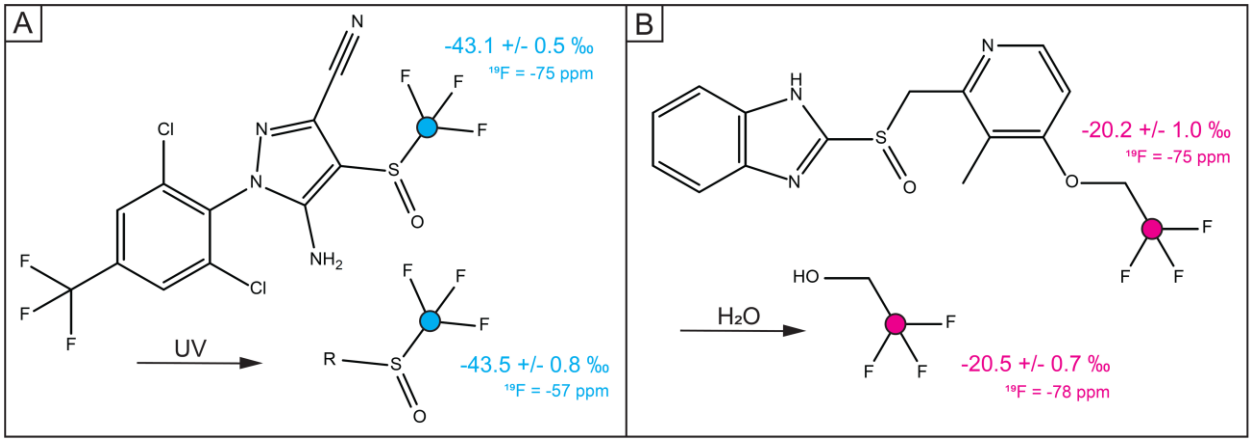

Figure 4: (A) The $^{13}C/^{12}C$ abundance of -43 ‰ in the trifluoromethylsulfoxide group of fipronil is preserved in its degradation product; and (B) the degradation of lansoprazole, 2,2,2-trifluoroethanol, also carries the original $^{13}C/^{12}C$ abundance of -20 ‰.

The strength of the C-F bond can make routine isotope ratio mass spectrometry analysis of organofluorine compounds challenging, due to the difficulty achieving complete combustion of the sample. Recent advances have addressed this limitation using specialized combustion approaches, high-temperature reactors, oxidative agents, and combustion-ion chromatography workflows, providing stable isotope analysis of organofluorine compounds[37-39]. For example, Dombrowski et al.[37] developed a gas chromatography-combustion IRMS method to measure carbon isotope ratios in selected per- and polyfluoroalkyl substances (PFAS), revealing significant variability in $^{13}C/^{12}C$ abundance among the analyzed molecules. Similarly, Wojtal et al.[39] demonstrated the application of high-resolution mass spectrometry for precise carbon isotopic analysis of perfluorooctanoic acid. These studies report $^{13}C/^{12}C$ ratios which range from -27‰ to -46‰[37-39], consistent with those of petroleum-derived compounds[40]. PFAS are typically synthesized from precursors derived from crude oil or natural gas, and inherit their isotopically

light carbon signature from these fossil fuels, which originate from ancient biological carbon fixed via photosynthesis.

However, these IRMS-based methods provide only bulk or molecule-average isotope ratios, and therefore mask the wealth of information contained within the position-specific $^{13}C/^{12}C$ distribution. In contrast, position-specific carbon isotope information provides $^{13}C/^{12}C$ ratios at individual carbon sites, producing multiple observations per compound. Here we find that intramolecular carbon isotope variability can be quite significant and distinctive. For example, we found that Paxil tablets preserve an intramolecular $^{13}C/^{12}C$ abundance ranging from -32 ‰ to -52 ‰ (Figure 2), and $^{13}C/^{12}C$ abundance in lansoprazole ranges from -11 ‰ to -35 ‰ (Figure 3). The $^{13}C/^{12}C$ variability was a more modest ~5 ‰ in the two bifenthrin samples analyzed (Figure S8). These position-specific isotope patterns may be imprinted by precursors and/or synthesis methods, and can help in distinguishing chemically identical molecules that are the products of different manufacturing routes or transformation processes.

PFAS with long perfluoroalkyl chains are also of interest due to their persistence in the environment[1,7,11-17]. These higher molecular weight PFAS can pose challenges for $^{13}C/^{12}C$ analysis via ^{19}F NMR, due to spectral overlap among chemically similar CF_2 units. However, some subset of the resonances in long-chain PFAS, such as the terminal CF_3 and other chemically distinctive groups, may be well enough resolved to be amenable to $^{13}C/^{12}C$ analysis using the methods described here.

The ^{19}F and ^{1}H NMR spectra in this work are acquired under fully relaxed conditions, which is ideal for quantitative impurity profiling[26-28]. This approach provides an additional dimension to the isotopic fingerprint that is obtained from $^{13}C/^{12}C$ analysis. Impurity profiling enables the distinction of chemically identical compounds (*e.g.*, paroxetine or lansoprazole from different suppliers) by quantifying co-occurring impurities or companion molecules. Importantly, impurity profiling can be performed using the same spectra collected for $^{13}C/^{12}C$ analysis, and with high (sub-microgram) sensitivity. As a specific example, the spectra in Figure 1 were acquired using 20 mg of paroxetine; however, the $^{19}F–^{13}C$ satellite peaks arise from only ~1/180 of that mass (0.11 mg), yet still exhibit a signal-to-noise ratio greater than 100:1. The small impurities visible in Figures 1A and 1B have an abundance that is much lower than the satellite peaks, and have masses 1 to 10 microgram range; the signal-to-noise is the spectra is such that sub-microgram amounts can be detected. Comparison of the ^{13}C-coupled and ^{13}C-decoupled spectra allows minor impurities to be distinguished from ^{13}C satellites. We found that paroxetine and lansoprazole from different sources were each clearly distinguishable based on their microgram-scale impurity profiles (Figure S11), in addition to their position-specific $^{13}C/^{12}C$ isotope ratios. This combined isotope-impurity fingerprint adds an extra level of confidence in linking a molecule to its source.

CONCLUSION

This work demonstrates $^{13}C/^{12}C$ analysis via ^{19}F NMR as a tool for fingerprinting organofluorine compounds, within mixtures, despite the presence of overlapping ^{19}F NMR impurity signals. Potential applications include product validation, forensics, environmental tracing, including linking organofluorine compounds to their breakdown products. Results demonstrate that position-specific $^{13}C/^{12}C$ analysis via ^{19}F NMR can reveal significant intramolecular isotope variability that cannot be detected using traditional IRMS measurements. The ^{19}F NMR method offers another key advantages: It produces NMR spectra that are ideal for impurity profiling. A limitation of $^{13}C/^{12}C$ analysis via ^{19}F NMR is its sensitivity, compared to conventional IRMS. Rather than view NMR, IRMS and ^{19}F NMR-based impurity profiling as competing

techniques, these methods can be complementary tools for characterizing a sample and its degradation products.

Supporting Information

The Supporting information is available free of charge and includes additional figures, representative plotted NMR spectra of samples discussed in this work, examples of peak shape analyses for isotope ratio determinations, and a detailed description of the data collection and processing used to obtain $^{13}C/^{12}C$ isotope abundance (PDF). A table summarizing the results, raw NMR data and R-scripts used for processing the data are available for download from the Texas Date Repository at:
https://doi.org/10.18738/T8/S5ULX6

ACKNOWLEDGEMENTS
This material is based upon work supported by the U.S. Department of Energy, Office of Science, Office of Basic Energy Sciences, Geosciences program under Award Number DE-SC0022524.

Author Information

Corresponding author: David W. Hoffman, Department of Molecular Biosciences, College of Natural Science, University of Texas at Austin, 100 E 24th St, Austin, TX 78712. Orcid: 0002-4983-6912. Email: dhoffman@mail.utexas.edu

Author: Cornelia Rasmussen, University of Texas Institute for Geophysics, Jackson School of Geosciences, University of Texas at Austin, 10601 Exploration Way, Austin, TX 78758. crasmussen@utexas.edu

Notes

The authors declare no competing financial interest.

REFERENCES

1. Glüge, J.; Scheringer, M.; Cousins, I. T.; DeWitt, J. C.; Goldenman, G.; Herzke, D.; Lohmann, R.; Ng, C. A.; Trier, X.; Wang, Z. An Overview of the Uses of Per- and Polyfluoroalkyl Substances (PFAS). *Environ. Sci.: Processes Impacts* **2020**, *22* (12), 2345–2373.

2. Britton, R.; Gouverneur, V.; Lin, J. H.; Meanwell, M.; Ni, C.; Pupo, G.; Xiao, J.; Hu, J. Contemporary Synthetic Strategies in Organofluorine Chemistry. *Nat. Rev. Methods Primers* **2021**, *1* (1), 47.

3. Hagmann, W. K. The many roles for fluorine in medicinal chemistry. J. Med. Chem. **2008**, 51 (15), 4359−4369.

4. Purser, S.; Moore, P. R.; Swallow, S.; Gouverneur, V. Fluorine in medicinal chemistry. Chem. Soc. Rev. **2008**, 37 (2), 320−330.

5. Prakash, G.S. and Wang, F. Fluorine: the new kingpin of drug discovery. *chim. oggi/Chem. Today*, **2012**, *30*(5), 30-36.

6. Zhou, Y.; Wang, J.; Gu, Z.; Wang, S.; Zhu, W.; Aceña, J. L.; Soloshonok, V. A.; Izawa, K.; Liu, H. Next generation of fluorine-containing pharmaceuticals, compounds currently in phase II−III clinical trials of major pharmaceutical companies: new structural trends and therapeutic areas. *Chem. Rev.* **2016**, 116 (2), 422−518.

7. Wang, Z.; DeWitt, J. C.; Higgins, C. P.; Cousins, I. T. A Never-Ending Story of Per- and Polyfluoroalkyl Substances (PFASs)? *Environ. Sci. Technol.* **2017**, *51* (5), 2508–2518.

8. Jeschke, P. The unique role of fluorine in the design of active ingredients for modern crop protection. ChemBioChem 2004, 5 (5), 570−589.

9. Jeschke, P. The unique role of halogen substituents in the design of modern agrochemicals. Pest Manage. Sci. **2010**, 66 (1), 10−27.

10. Zhang, W.; Liang, Y. The Wide Presence of Fluorinated Compounds in Common Chemical Products and the Environment: A Review. *Environ. Sci. Pollut. Res.* **2023**, *30* (50), 108393–108410.

11. Ghisi, R.; Vamerali, T.; Manzetti, S. Accumulation of Perfluorinated Alkyl Substances (PFAS) in Agricultural Plants: A Review. *Environ. Res.* **2019**, *169*, 326–341.

12. Kwiatkowski, C. F.; Andrews, D. Q.; Birnbaum, L. S.; Bruton, T. A.; DeWitt, J. C.; Knappe, D. R. U.; Maffini, M. V.; Miller, M. F.; Pelch, K. E.; Reade, A.; Soehl, A.; Trier, X.; Venier, M.; Milkov, A. V.; Schwietzke, S.; Allen, G.; Sherwood, O. A.; Etiope, G. Using Global Isotopic Data to Constrain the Role of Shale Gas Production in Recent Increases in Atmospheric Methane. *Sci. Rep.* **2020**, *10* (1), 4199.

13. Gagliano, E.; Sgroi, M.; Falciglia, P. P.; Vagliasindi, F. G.; Roccaro, P. Removal of Poly- and Perfluoroalkyl Substances (PFAS) from Water by Adsorption: Role of PFAS Chain Length, Effect of Organic Matter, and Challenges in Adsorbent Regeneration. *Water Res.* **2020**, *171*, 115381.

14. Cousins, I. T.; Johansson, J. H.; Salter, M. E.; Sha, B.; Scheringer, M. Outside the Safe Operating Space of a New Planetary Boundary for Per- and Polyfluoroalkyl Substances (PFAS). *Environ. Sci. Technol.* **2022**, *56* (16), 11172–11179.

15. Dickman, R. A.; Aga, D. S. A Review of Recent Studies on Toxicity, Sequestration, and Degradation of Per- and Polyfluoroalkyl Substances (PFAS). *J. Hazard. Mater.* **2022**, *436*, 129120.

16. Espartero, L. J. L.; Yamada, M.; Ford, J.; Owens, G.; Prow, T.; Juhasz, A. Health-Related Toxicity of Emerging Per- and Polyfluoroalkyl Substances: Comparison to Legacy PFOS and PFOA. *Environ. Res.* **2022**, *212*, 113431.

17. Bline, A.; DeWitt, J.; Kwiatkowski, C.; Pelch, K.; Reade, A.; Varshavsky, J. Public Health Risks of PFAS-Related Immunotoxicity Are Real. *Curr. Environ. Health Rep.* **2024**, *11* (2), 118–127. https://doi.org/10.1007/s40572-024-00441-y

18. Göckener, B.; Weber, T.; Rüdel, H.; Bücking, M.; Kolossa-Gehring, M. Human Biomonitoring of Per- and Polyfluoroalkyl Substances in German Blood Plasma Samples from 1982 to 2019. *Environ. Int.* **2020**, *145*, 106123.

19. De Silva, A. O.; Armitage, J. M.; Bruton, T. A.; Dassuncao, C.; Heiger-Bernays, W.; Higgins, C. P.; et al. PFAS Exposure Pathways for Humans and Wildlife: A Synthesis of Current Knowledge and Key Gaps in Understanding. *Environ. Toxicol. Chem.* **2021**, *40*, 631–657.

20. Lauria, M. Z.; Shi, X.; Haque, F.; Plassmann, M.; Roos, A.; Simon, M.; Benskin, J. P.; Jobst, K. J. Discovery of Fluorotelomer Sulfones in the Blubber of Greenland Killer Whales (*Orcinus orca*). *Environ. Sci. Technol. Lett.* **2025**, *12* (9), 1218–1224.

21. Neubauer, C.; Sweredoski, M. J.; Moradian, A.; Newman, D. K.; Robins, R. J.; Eiler, J. M. Scanning the Isotopic Structure of Molecules by Tandem Mass Spectrometry. *Int. J. Mass Spectrom.* **2018**, *434*, 276–286.

22. Rasmussen, C.; Hoffman, D. W. Intramolecular Distribution of $^{13}C/^{12}C$ Isotopes in Amino Acids of Diverse Origins. *Amino Acids* **2020**, *52* (6–7), 955–964.

23. Rasmussen, C.; Hoffman, D. W. Novel Nuclear Magnetic Resonance Method for Position-Specific Carbon Isotope Analysis of Organic Molecules with Significant Impurities. *Anal. Chem.* **2022**, *94* (43), 15124–15131.

24. Hoffman, D. W.; Rasmussen, C. Position-Specific Carbon Stable Isotope Analysis of Glyphosate: Isotope Fingerprinting of Molecules within a Mixture. *Anal. Bioanal. Chem.* **2024**, *416* (16), 3847–3856.

25. Remaud, G. S.; Akoka, S. A Review of Flavors Authentication by Position-Specific Isotope Analysis by Nuclear Magnetic Resonance Spectrometry: The Example of Vanillin. *Flavour Fragrance J.* **2017**, *32* (2), 77–84.

26. Mistry, N.; Ismail, I.M.; Farrant, R.D.; Liu, M.; Nicholson, J.K.; Lindon, J.C. Impurity profiling in bulk pharmaceutical batches using 19F NMR spectroscopy and distinction between monomeric and dimeric impurities by NMR-based diffusion measurements. *Journal of pharmaceutical and biomedical analysis*, **1999**, *19*(3-4), 511-517.

27. Okaru, A.O.; Brunner, T.S.; Ackermann, S.M.; Kuballa, T.; Walch, S.G.; Kohl-Himmelseher, M.; Lachenmeier, D.W. Application of 19F NMR spectroscopy for content determination of fluorinated pharmaceuticals. *Journal of analytical methods in chemistry*, **2017,** (1) 9206297.

28. Liu, C.M.; Song, C.H., Jia, W.; Hua, Z.D.; Liao, Q. The application of ^{19}F NMR spectroscopy for the analysis of fluorinated new psychoactive substances (NPS). *Forensic Science International,* **2022**, *340*, 111450.

29. Xu, Z., Gu, S., Li, Y., Wu, J., Zhao, Y., Recognition-enabled automated analyte identification via ^{19}F NMR. Analytical Chemistry **2022**, 94(23), 8285-8292.

30. Gauthier, J. R.; Mabury, S. A. Identifying unknown fluorine-containing compounds in environmental samples using ^{19}F NMR and spectral database matching. *Environ. Sci. Technol.* **2023**, 57 (23), 8760−8767.

31. Camdzic, D.; Dickman, R. A.; Joyce, A. S.; Wallace, J. S.; Ferguson, P. L.; Aga, D. S. Quantitation of Total PFAS Including Trifluoroacetic Acid with Fluorine Nuclear Magnetic Resonance Spectroscopy. Anal. Chem. **2023**, 95(13), 5484–5488.

32. Rasmussen, C.; Hoffman, D. Fingerprinting Organofluorine Molecules via Position-Specific Isotope Analysis. *Environ. Sci. Technol.* **2024**, *58* (30), 13426–13433.

33. Willcott, M. R. MestRe Nova. *J. Am. Chem. Soc.* **2009**, *131* (36), 13180.

34. Holtvoeth, J.; Whiteside, J. H.; Engels, S.; Freitas, F. S.; Grice, K.; Greenwood, P.; Sepúlveda, J. The Paleolimnologist's Guide to Compound-Specific Stable Isotope Analysis-An Introduction to Principles and Applications of CSIA for Quaternary Lake Sediments. *Quat. Sci. Rev.* **2019**, *207*, 101–133.

35. Hoffman, D.W.; Rasmussen, C. Absolute carbon stable isotope ratio in the Vienna Peedee Belemnite isotope reference determined by ^{1}H NMR spectroscopy. *Analytical Chemistry* **2022**, *94*(13), 5240-5247.

36. Raveton, M.; Aajoud, A.; Willison, J. C.; Aouadi, H.; Tissut, M.; Ravanel, P. Phototransformation of the Insecticide Fipronil: Identification of Novel Photoproducts and Evidence for an Alternative Pathway of Photodegradation. *Environ. Sci. Technol.* **2006**, *40* (13), 4151–4157.

37. Dombrowski, A.; Wojtal, P. K.; Pan, H.; Lane, C. S.; Mead, R. N. Stable Carbon and Sulfur Isotopic Compositions of Per- and Polyfluoroalkyl Substances. *Environ. Sci. Technol. Lett.* **2025**, *12* (2), 216–221.

38. Di Marcantonio, E.; Shouakar-Stash, O.; Marchesi, M.; Dallai, L. Compound-Specific Carbon Isotope Analysis of Perfluorocarboxylic Acids (PFCAs) by Gas Chromatography-Isotope Ratio Mass Spectrometry. *Sci. Total Environ.* **2025**, *1001*, 180564.

39. Wojtal, P. K.; Davidheiser-Kroll, B.; Lane, C. S.; Mead, R. N. Stable Carbon Isotope Analysis of Perfluorooctanoic Acid (PFOA) by Microflow-High-Pressure Liquid Chromatography–Orbitrap Mass Spectrometry. *Rapid Commun. Mass Spectrom.* **2025**, *39* (24), e10139.

40. Ogbesejana, A. B.; Liu, B.; Ostadhassan, M. Stable Isotope Geochemistry of the Organic Elements within Shales and Crude Oils: A Comprehensive Review. *Molecules* **2021**, *27* (1), 34.